RESEARCH PAPER | Science | Volume : 4 | Issue : 5 | May 2014 | ISSN - 2249-555X

The Study of Bronze Behaviour During Cavitation Erosion

KEYWORDS: cavitation erosion; aluminium bronze; pump rotor

Cinca Ionel Lupinca
Eftimie Murgu University of Resita, Traian Vuia Sq., No. 1-4, Resita, Romania

Marian Dumitru Nedeloni
Eftimie Murgu University of Resita, Traian Vuia Sq., No. 1-4, Resita, Romania

ABSTRACT *The behaviour of aluminium bronze to cavitation erosion represents the main objective of this paper. In order to analyze the behaviour during cavitation erosion of castings resulted from alloys like Cu-Al, Cu-Al-Fe and Cu-Sn-Pb specimens with sides of 16x16x10 mm were used. These specimens were taken from cast samples in order to determine mechanical trial on the charge. The study was based on the application of an indirect method to determine the resistance to cavitation erosion of these specimens. The results of the study offer the necessary information for the exploitation of castings realized from the non-ferrous alloys mentioned.*

INTRODUCTION

According to technical-scientific information it is well known that aluminium bronzes are often used for the production of castings like water pumps rotors, bearings, piston rods, glides and other castings that are resistant to corrosion and with antifriction properties

Whereas lead bronzes are frequently used to cast bearings for motor parts with an internal combustion and the results of the study regarding the behaviour to cavitation erosion are used for a comparative analysis with aluminium bronzes.

Taking into consideration the behaviour to cavitation erosion of castings realized from copper - based alloys as being dependent on the structure of solid state alloys, respectively on the phases and the metallographic constituents, a study of the metallographic structure of these alloys will also be presented. The presence of non-metallic inclusions in the structure presenting the tendency of separation, during solidification at the limit between grains of the alpha solid solution have a strong influence on the castings behaviour during cavitation erosion.

Table 1 presents the chemical compositions prescribed for copper-based alloys [5], and Table 2, the chemical compositions of copper based alloys obtained from castings.

The paper contains the results of experiments realized at the "Eftimie Murgu" University of Resita on the behaviour to cavitation erosion of specimens taken from castings realized from copper based alloys.

EXPERIMENTAL RESULTS

1. DETERMINATION OF PARAMETERS

The testing during cavitation erosion of these bronze specimens was realized with the help of a vibrator composed of: an ultrasound generator, a piezoelectric enhancer, an acoustic concentrator, a sontrode, the liquid vessel and the specimens.

TABLE - 1 CHEMICAL COMPOSITION PRESCRIBED FOR COPPER ALLOYS [5]

Alloy type	Cu	Sn	Pb	Al	Fe	Ni	Zn	Mn	Si	Mg/P	Sb
CuAl9	Rest	Max. 0.25	Max. 0.25	8.2-10.5	Max. 1.0	Max. 1.0	Max. 0.4	Max. 0.50	Max. 0.20	-	-
CuAl10Fe2	83.0-89.5	Max. 0.20	Max. 0.10	8.5-10.5	1.5-3.3	Max. 1.5	Max. 0.50	Max. 1.0	Max. 0.20	Mg_{max} 0.05	-
CuSn7Pb15	74.0-80.0	6.0-8.0	13.0-17.0	Max. 0.01	Max. 0.25	0.5-2.0	Max. 2.0	Max. 0.20	Max. 0.01	P_{max} 0.10	Max. 0.50

TABLE - 2 CHEMICAL COMPOSITION REALIZED FOR COPPER ALLOYS USED FOR CASTINGS [3]

Copper alloy type	Cu	Al	Pb	Fe	Sn	Zn	Ni	Mn
CuAl9	88.9	10.3	0.09	0.46	<0.02	<0.04	<0.02	<0.001
CuAl10Fe2	85.1	10.4	<0.02	3.76	<0.02	<0.04	0.51	0.15
CuSn7Pb15	77.1	<0.006	14.8	<0.10	7.85	<0.004	0.18	-

Volume : 4 | Issue : 5 | May 2014 | ISSN - 2249-555X

For the proper trials of cavitation erosion, the indirect cavitation methods was used, the specimens tested (16 x 16 x 10) being fixed on an axle bracket, and the distance between the sontrode and the specimen being of 0.6 mm.

The testing was realized according to standards G32-10 [6] and G32-92 [7] regarding the cavitation method. The values of parameters for the vibrator were set at 20 ± 0.1 kHz, regarding the frequency and at 50 μm, for the amplitude and in order to measure the loss of specimen mass a digital scales was used with a reading capacity of 0.01 mg.

TABLE - 3 VALUES OBTAINED FOR THE ALLOY CuAl9

Accumul. time t [min]	Period, Δt [min]	Specimen mass, m [mg]	Eroded mass		Cavitation erosion rate, v_{ce}	
			Per / period, Δm [mg]	Accumulated, m_c [mg]	[mg/min]	[mg/h]
0	0	31490.57	0	0	0.0000	0.000
10	10	31490.17	0.4	0.4	0.0277	1.660
30	20	31490.11	0.06	0.46	0.0029	0.172
60	30	31490.03	0.08	0.54	0.0047	0.280
90	30	31489.83	0.2	0.74	0.0127	0.760
120	30	31489.27	0.56	1.3	0.0280	1.680
150	30	31488.15	1.12	2.42	0.0448	2.690
180	30	31486.58	1.57	3.99	0.0703	4.220
210	30	31483.93	2.65	6.64	0.0897	5.380
240	30	31481.2	2.73	9.37	0.0967	5.800
270	30	31478.13	3.07	12.44	0.1028	6.170
300	30	31475.03	3.1	15.54	0.1055	6.330
330	30	31471.8	3.23	18.77	0.1132	6.790
360	30	31468.24	3.56	22.33	0.1242	7.450

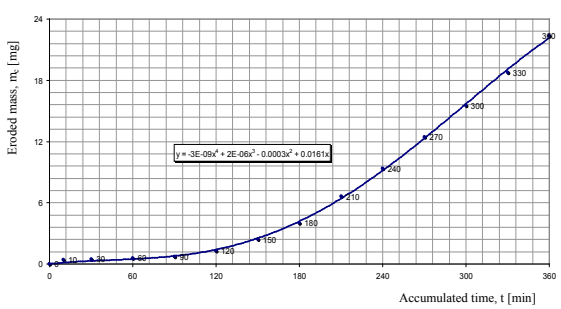

Figure 1: Material loss curve for CuAl9 alloy

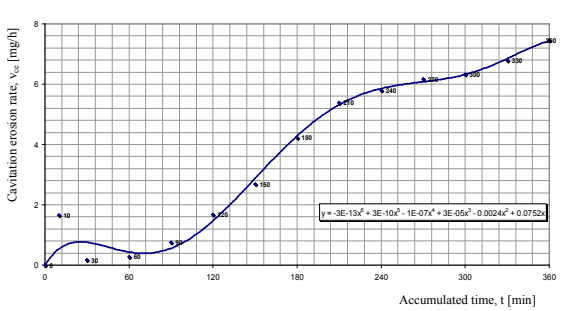

Figure 2: Cavitation erosion rate curve for CuAl9 alloy

For the types of bronzes studied, in Tables 3 ÷ 5, the values obtained for an accumulated time of 360 minutes of testing, are presented, and in figures 1, 3 and 5, the graphic representation of cumulates masses of material eroded through cavitation and in figures 2, 4 and 6, the erosion rates.

TABLE - 4 VALUES OBTAINED FOR THE ALLOY CuAl0Fe2

Accumul. time t [min]	Period, Δt [min]	Specimen mass, m [mg]	Eroded mass		Cavitation erosion rate, v_{ce}	
			Per / period, Δm [mg]	Accumulated, m_c [mg]	[mg/min]	[mg/h]
0	0	28589.09	0	0	0.0000	0.000
10	10	28588.97	0.12	0.12	0.0092	0.550
30	20	28588.9	0.07	0.19	0.0040	0.238
60	30	28588.76	0.14	0.33	0.0065	0.390
90	30	28588.51	0.25	0.58	0.0088	0.530
120	30	28588.23	0.28	0.86	0.0098	0.590
150	30	28587.92	0.31	1.17	0.0155	0.930
180	30	28587.3	0.62	1.79	0.0265	1.590
210	30	28586.33	0.97	2.76	0.0312	1.870
240	30	28585.43	0.9	3.66	0.0455	2.730
270	30	28583.6	1.83	5.49	0.0540	3.240
300	30	28582.19	1.41	6.9	0.0545	3.270
330	30	28580.33	1.86	8.76	0.0540	3.240
360	30	28578.95	1.38	10.14	0.0380	2.280

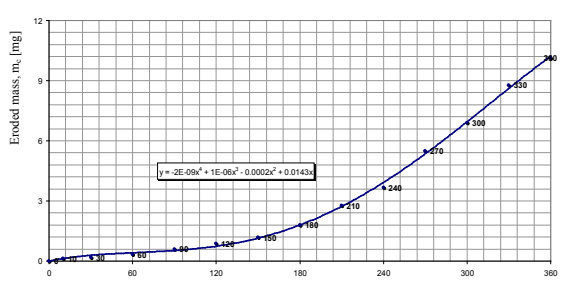

Figure 3: Material loss curve for CuAl10Fe2 alloy

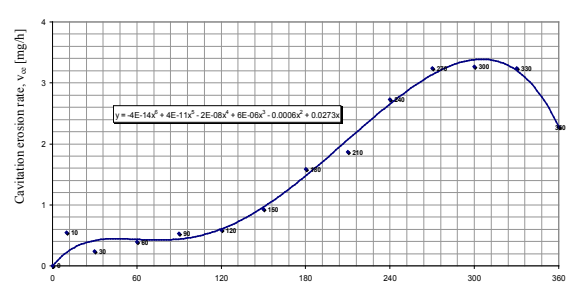

Figure 4: Cavitation erosion rate curve for CuAl10Fe2 alloy

Volume : 4 | Issue : 5 | May 2014 | ISSN - 2249-555X

TABLE - 5 VALUES OBTAINED FOR THE ALLOY CuSn-7Pb15

Accumul. time t [min]	Period, Δt [min]	Specimen mass, m [mg]	Eroded mass		Cavitation erosion rate, v_{ce}	
			Per / period, Δm [mg]	Accumulated, m_c [mg]	[mg/min]	[mg/h]
0	0	33729.08	0	0	0.0000	0.000
10	10	33727.24	1.84	1.84	0.1890	11.340
30	20	33723.26	3.98	5.82	0.1790	10.740
60	30	33718.79	4.47	10.29	0.2510	15.060
90	30	33708.2	10.59	20.88	0.4287	25.720
120	30	33693.07	15.13	36.01	0.5135	30.810
150	30	33677.39	15.68	51.69	0.4798	28.790
180	30	33664.28	13.11	64.8	0.4958	29.750
210	30	33647.64	16.64	81.44	0.4613	27.680
240	30	33636.6	11.04	92.48	0.4927	29.560
270	30	33618.08	18.52	111	0.5038	30.230
300	30	33606.37	11.71	122.71	0.4827	28.960
330	30	33589.12	17.25	139.96	0.4707	28.240
360	30	33578.13	10.99	150.95	0.2620	15.720

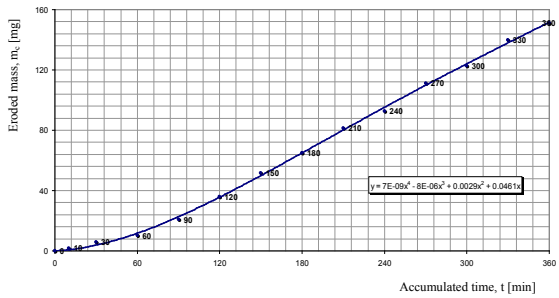

Figure 5: Material loss curve for CuSn7Pb15 alloy

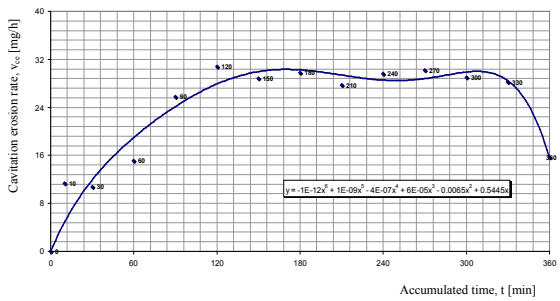

Figure 6: Cavitation erosion rate curve for CuSn7Pb15 alloy

Comments:

In the case of each of the three specimens of copper-based alloys subjected to trials of resistance to cavitation erosion, the mass loss during the period of the experiments increased exponentially, so that at the end of the testing (after 360 minutes) the following results to be obtained (in decreasing order): 150.59 mg, CuSn7Pb15, 22.33 mg, CuAl9 and 10.14 mg, CuAl10Fe2. Thus, the data presented highlight the fact that the most eroded material is the specimen CuSn8Pb15, and the least eroded that of the specimen from CuAl10Fe2.

2. THE ASPECTS OF THE SURFACES OF ERODED SPECIMENS

In figures 7÷9, the surfaces of frontal surfaces of specimens from copper alloys eroded by cavitation are presented after: 60 (a), 180 (b) and 360 minutes (c) of testing. Microstructural photos were realized with a photo camera with the help of the stereo-microscope.

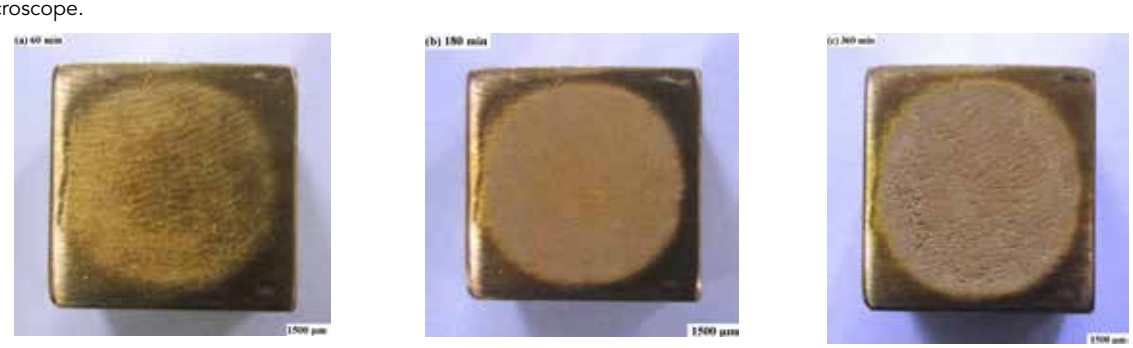

a. **b.** **c.**

Figure 7: The aspect of specimen surface from CuAl9 after: 60 min. (a), 180 min. (b) and 360 min. (c), of cavitation erosion

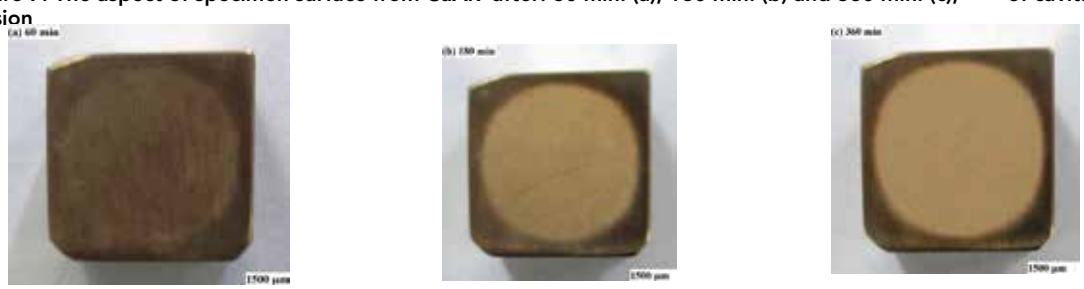

a. **b.** **c.**

Figure 8: The aspect of specimen surface from CuAl10Fe2 after: 60 min. (a), 180 min. (b) and 360 min. (c), of cavitation erosion

Volume : 4 | Issue : 5 | May 2014 | ISSN - 2249-555X

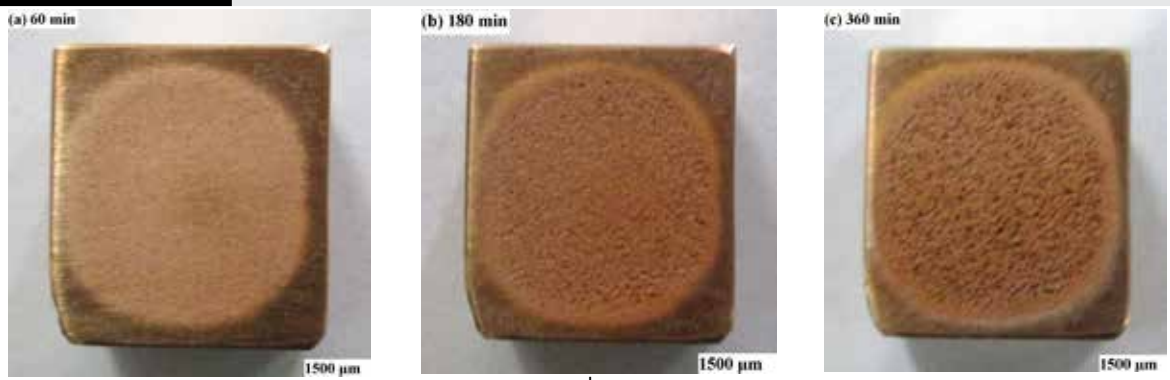

a. b. c.

Figure 9: The aspect of specimen surface from CuSn7Pb15 after: 60 min. (a), 180 min. (b) and 360 min. (c), of cavitation erosion

3. METALLOGRAPHIC STRUCTURES

In figures 10-12 the metallographic structures of copper alloys are presented, realized on specimens subjected to cavitation erosion tests.

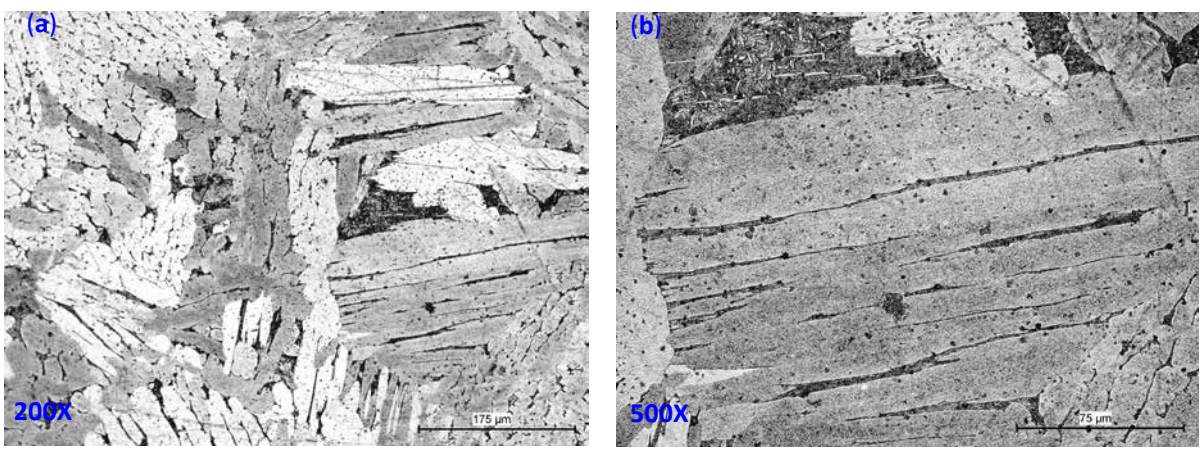

Figure 10: Metallographic structures of the specimen CuAl9

In the structure of the CuAl9 allow the α solution can be observes as being isomorphic with copper, the α solid solution and the intermetallic compound α_2 ($Cu_{32}Al_{19}$), resulted from an eutectoid decomposition of the α phase, at a temperature of 565°C. The grains of the solid solution have pretty large sizes, which denote the fact that the alloy wasn't modified properly.

The intermetallic compound $Cu_{32}Al_{19}$ (rough and fragile) can be found separately at the limit of grains from the α solid solution under the shape of strips and of small inclusions, but also pointform even in the interior of the solid solution grains.

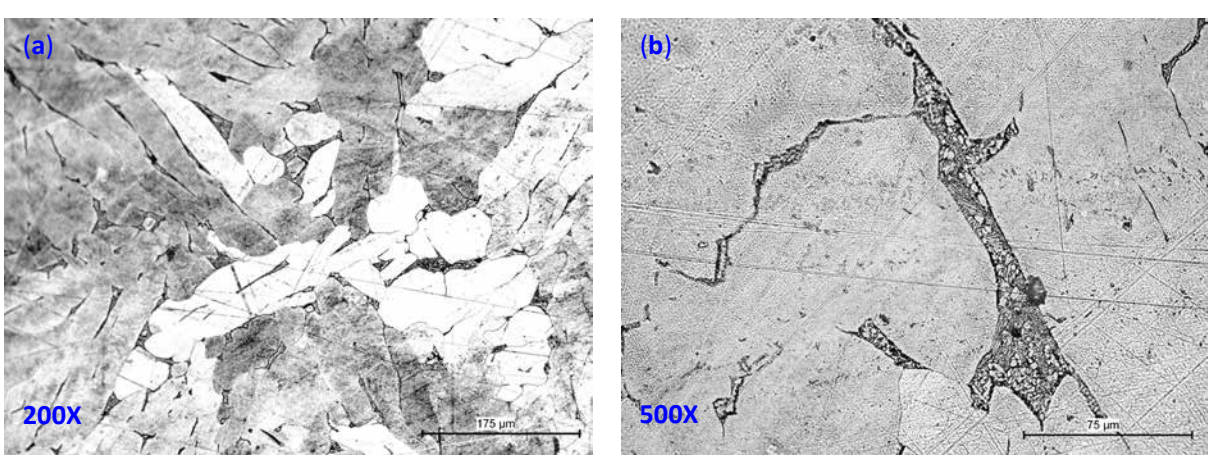

Figure 11: Metallographic structures of the specimen CuAl10Fe2

In the structure of the alloy CuAl10Fe2, the existence of the α solid solution can also be observed, but in more reduced sizes which proves the fact that the realization of a proper modification is proved by the iron added for the alloy alloying.

Volume : 4 | Issue : 5 | May 2014 | ISSN - 2249-555X

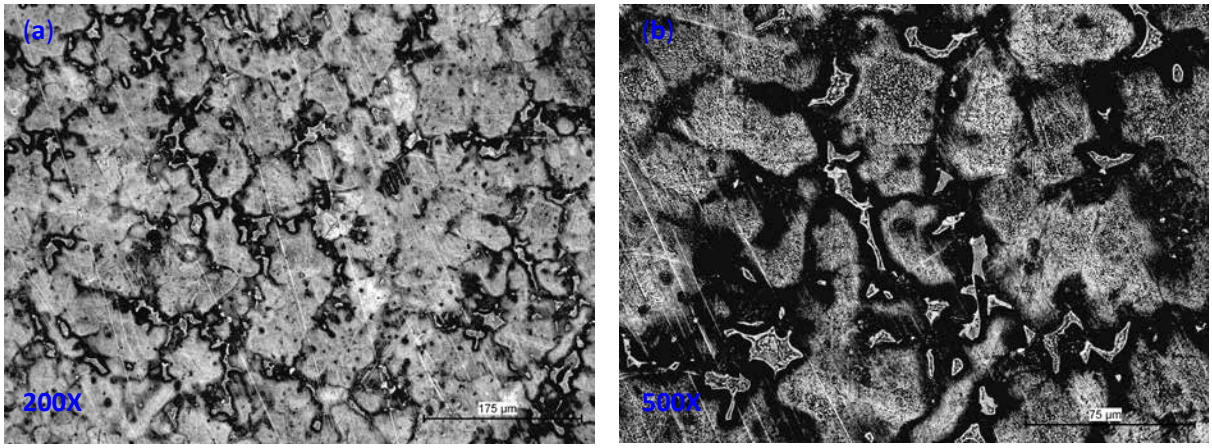

Figure 12: Metallographic structures of the specimen CuSn7Pb15

The structure of the alloy CuSn7Pb15 is characterized by pronounced lead separations at the limit of crystalline grains, forming an almost continuous network around them, as a result of its insolubility in copper. The matrix is in general composed of grains regulated in α solid solution.

CONCLUSIONS

- The study of graphics that underline the mass loses during the entire experiment (360 minute), but also the stereo-micrographs realized on eroded surfaces

In this case the intermetallic compound $Cu_{32}Al_{19}$ is seem as being less distributed in the interior of crystals of sold solution, but the its separation under the shape of networks can be observed to be on most of the times large, at the limit of crystals in the solid solution.

through cavitation underlined the following: the most non-ferrous eroded material, from the bronze category is the alloy Cu-Pb-Sn (CuSn7Pb15) in which the greatest accumulated mass loss was observed - 150,59 mg; the less eroded non-ferrous material is the alloy Cu-Al-Fe for which the accumulated mass lost during the same period was of 10,14 mg. In this case, the accumulated mass loss was of almost 15 smaller for the alloy Cu-Al-Fe in comparison to the alloy Cu-Pb-Sn.

- Between the two non-ferrous alloys based on copper from the same category (Cu-Al alloy), respectively non-ferrous alloys: CuAl9 and CuAl10Fe2 a similitude with the previous case has been observed, but at a smaller scale. Thus the alloy CuAl10Fe2 (10.14 mg, accumulated mass loss) is corroded by erosion twice less than the alloy CuAl9 (22.33 mg, accumulated mass loss).

- From a structural point of view, all three types of alloys based on copper are present in the α solid structure, isomorphic with copper; the most significant presence of the intermetallic compound $Cu_{32}Al_{19}$ (Phase α_2) (resulted from the eutectic decomposition of the α phase), as isolated inclusions is found in grains and at the limit of grains of α solid solution is observed in the alloy CuAl9; in the alloy CuAl10Fe2, this intermetallic compound forms a small interrupted network around the crystalline grains from the α solid solution.

- Also, the alloy CuAl10Fe2 presents a modified structure resulted from the actions realized by the iron in the composition. According to theories that explain the modifications applied to all categories of alloys, by modification, a slight increase of the modified material hardness if obtained.

- If Brinell hardness if compared and as suggested by in force standards [3] these show higher values for the alloy for the casting process.

According to these statements it can be proved why in the case of non-ferrous alloys based on copper the alloy Cu-Pb-Sn behaves like a soft material in the conditions of cavitation erosion, the best behaviour is observed in the alloy Cu-Sn-Fe, in the same conditions.

REFERENCE [1]Ghiban, B., Mânzâna, M.E., Bordeasu, I., Ghiban, N., Marin, M. (2010), "Structural analysis for brase and bronze through cavitation", Scientific Bulletin of the "Politehnica" University of Timisoara, Transactions on Mechanics, vol. 55 (68), Romania, pp. 63÷66. | [2]Nedeloni, M.D., Nedelcu, D. (2012), "Variants of sonotrode for vibratory apparatus for test cavitation erosion by the indirect method", Constanta Maritime University Annals, no. 17, Year XII, July, Romania. | [3] Nedeloni, M.D., Nedelcu, D. (2012), Research through Direct and Indirect Cavitaion method for a Aluminium Specimen, Annals of "Eftimie Murgu" University, vol. XIX, No. 1, Resita, Romania. | [4]Tang, C.H., Cheng, F.T., Man, H.C. (2004), Improvement in cavitation erosion resistance of copper-based propeller alloy by laser surface melting, Surface and Coatings technology, no. 182, pp. 300÷307. | [5] *** SR EN 1982 (2008), Cooper and copper alloys. Ingots and castings, ASRO Standard, Romania. | [6] *** ASTM Standard G32-92 (1992), Standard Method of Vibratory Cavitation Erosion Test. Annual Book of ASTM Standards, Philadelphia, United States. | [7] *** ASTM G32 – 10 (2010), Standard Test Method for Cavitation Erosion Using Vibratory Apparatus, Copyright © ASTM International, United States. |